

1 **WET SCRUBBING INTENSIFICATION APPLIED TO HYDROGEN**  
2 **SULPHIDE REMOVAL IN WASTE WATER TREATMENT PLANT**

3  
4  
5 **Pierre-François Biard<sup>a,b,c\*</sup>, Annabelle Couvert<sup>b,c</sup>, Christophe Renner<sup>a</sup>, Jean-**  
6 **Pierre Levasseur<sup>d</sup>**

7  
8 *<sup>a</sup>Anjou Recherche-Veolia Environnement, Chemin de la Digue, BP 76, 78603*  
9 *Maisons-Laffitte, France*

10 *<sup>b</sup>Ecole Nationale Supérieure de Chimie de Rennes, CNRS, UMR 6226, Avenue du*  
11 *Général Leclerc, CS 50837, 35708 Rennes Cedex 7, France*

12 *<sup>c</sup>Université européenne de Bretagne*

13 *<sup>d</sup>Veolia Water, Direction Technique, 1 rue Giovanni Battista Pirelli, 94410 Saint-*  
14 *Maurice, France*

---

\* Corresponding author: Tel: +33 2 23 23 81 57 / Fax: + 33 2 23 23 81 20

*Email address : pierre-francois.biard@ensc-rennes.fr*

16           **Abstract**

17           Hydrogen sulphide removal in a Waste Water Treatment Plant at semi-industrial scale  
18 in a compact wet scrubber has been investigated. The gas residence time in the scrubber was  
19 reduced to 30 ms using a NaOCl caustic scrubbing solution. The contactor is composed of a  
20 wire mesh packing structure where liquid and gas flow co-currently at high velocity ( $> 12$   
21  $\text{m.s}^{-1}$ ).  $\text{H}_2\text{S}$  removal percentages higher than 95% could be achieved whereas a moderate  
22 pressure drop was measured ( $< 4000$  Pa). Both the hydrodynamic and chemical conditions  
23 can influence the efficiency of the process. Correlations were developed to predict both the  
24 pressure drop and the  $\text{H}_2\text{S}$  removal efficiency at given operating conditions.

25

26           **Résumé**

27           Le traitement du sulfure d'hydrogène dans un laveur de gaz compact a été étudié à  
28 l'échelle semi-industrielle en station d'épuration. Le temps de contact dans le laveur est réduit  
29 à une trentaine de ms en utilisant une solution d'hypochlorite de sodium à pH basique. Le  
30 contacteur se compose d'une structure tissée métallique dans laquelle le gaz et le liquide  
31 circulent à co-courant et grande vitesse ( $> 12 \text{ m.s}^{-1}$ ). Un abattement de l' $\text{H}_2\text{S}$  de plus de 95%  
32 peut être obtenu avec une perte de charge modérée ( $< 4000$  Pa). A la fois les conditions  
33 chimiques et hydrodynamiques influencent les performances de traitement. Des corrélations  
34 ont été développées pour prédire la perte de charge mais aussi l'abattement dans des  
35 conditions opératoires données.

36

37           **Keywords:** Absorption, chemical scrubbing, compact scrubber, hydrogen sulphide,  
38 odour control.

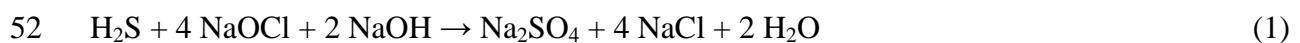
39

## 40 INTRODUCTION

41

42 Hydrogen sulphide is the major compound involved in odour emissions from WWTPs  
43 (Gostelow, 2001). The strategy applied in WWTPs to reduce odour emissions consists to  
44 ventilate the odorous stages (pre-treatment, biological aeration, sludge treatment, etc) and to  
45 bring the collected air into a single odour control unit in which different processes can be  
46 implemented (Busca and Chiara, 2003). The most common process used is the packed towers,  
47 in which pollutants are removed by chemical scrubbing (Bonnin, 1991 ; Chen et al., 2001).  
48 Chemical scrubbing involves pollutant mass transfer in an aqueous phase and subsequent  
49 reactions with acidic, basic or oxidant reagent(s). Most of the time, H<sub>2</sub>S is oxidised by sodium  
50 hypochlorite (NaClO) in an alkaline solution (pH ≥ 9):

51



53

54 H<sub>2</sub>S consumption in the liquid phase allows to maintain a driving force in order to  
55 achieve mass transfer. Moreover, when the reaction kinetics is fast compared to the mass  
56 transfer kinetics, mass transfer enhancement is involved.

57 Chemical scrubbing in packed towers has revealed high investment and operating  
58 costs (Couvert et al., 2008). Indeed, it implies the construction of high and large wet  
59 scrubbers. Moreover, long and expensive pipes and powerful fans are necessary to bring the  
60 waste air to the odour control unit. An alternative leading to the reduction of investment and  
61 operating costs could consist in treating odorous gas near each emission source in compact  
62 scrubbers in which the fluid residence time is significantly shorter. Process intensification,  
63 through mass transfer and superficial velocity enhancement inside the contactor, allows to  
64 decrease the reactor size and the fluid residence time.

65           The key element of the new Aquilair Plus<sup>TM</sup> process is a patented high voidage  
66 contactor specially adapted to compact wet scrubbing (Sanchez et al., 2007a ; Biard et al.,  
67 2009a). This down flow co-current contactor consists of a wire mesh packing structure where  
68 gas flows at high velocity ( $U_{SG} > 12 \text{ m}\cdot\text{s}^{-1}$ ). The liquid, swept along by the gas, collides with  
69 the wire mesh and is dispersed into fine droplets. At the laboratory scale, high mass transfer  
70 rate has been demonstrated for a moderate pressure drop (Sanchez et al., 2007b). The gas  
71 residence time could be reduced to less than 50 ms instead of about 1 or 2 seconds in packed  
72 towers to treat  $\text{H}_2\text{S}$  (Sanchez et al., 2007c). At the laboratory scale, an increase of the  
73 superficial gas velocity ( $U_{SG}$ ) and in a minor extent of the superficial liquid velocity ( $U_{SL}$ ) led  
74 to better interfacial area ( $a^0$ ) and gas and liquid mass transfer coefficients ( $k_{GA}^0$  and  $k_{LA}^0$ ) due  
75 to a higher energy loss (Sanchez et al., 2007b ; Biard et al., 2009b).

76           The aim of this study was to test the potentialities of the process at the semi-industrial  
77 scale (designed to treat gas flow rates  $Q_G$  ranging between 1500 and 2000  $\text{m}^3\cdot\text{h}^{-1}$ ) with a real  
78 gaseous effluent extracted from a WWTP. Scale-up difficulty is due to wall effects reduction  
79 at larger contactor sizes, which can induce both lower liquid dispersion and mass transfer rate.  
80 Between the laboratory and the semi-industrial scales, the spatial disposition of the wire  
81 meshes was modified to provide higher tortuosity. Both the pressure drop ( $\Delta P$ ) and the  $\text{H}_2\text{S}$   
82 removal percentage were determined versus several parameters. The influence of the  
83 superficial gas velocity ( $U_{SG}$ ), the superficial liquid velocity ( $U_{SL}$ ), the pH, the sodium  
84 hypochlorite concentration of the scrubbing liquid ( $[\text{ClO}^-]$ ) and the  $\text{H}_2\text{S}$  inlet concentration  
85 ( $[\text{H}_2\text{S}]_{G,i}$ ) was characterised. A model was developed in order to predict  $\text{H}_2\text{S}$  removal  
86 efficiency and pressure drop in the scrubber.

87

88

## 89 MATERIALS AND METHODS

90

91 The contactor is composed of a wire mesh structure of 200 mm diameter (void fraction  
92  $\approx 99.0\%$ ). The initial height ( $H_r$ ) of the packing was 600 mm but after the first experiments,  
93 the packing was compressed to 500 mm. The polluted air was pumped from the extraction  
94 pipe of the WWTP with a fan (AEIB) (Figure 1). By opening a valve placed before the fan, it  
95 was possible to dilute polluted air with clean air to modify the inlet  $H_2S$  concentration  
96 ( $[H_2S]_{G,i}$  in ppmv: Part Per Million by Volume). The gas flow rate  $Q_G$  was measured and  
97 controlled by means of a Pitot Tube (Deltabar S PMD 70 from Endress Hauser) and a  
98 frequency variator (Allen Bradley). The liquid injection upstream the contactor was insured  
99 by a spray nozzle SpiralJet (Spraying System). A 400 L tank allowing to store the scrubbing  
100 liquid and to separate the gas-liquid mixture was placed downstream the contactor. A droplet  
101 separator was placed downstream the tank before emission in atmosphere (Horus  
102 Environnement). The storage tank was filled with ground water previously softened. Reagents  
103 (NaOCl and NaOH provided by Brenntag) were pumped from 1000 L tanks to the storage  
104 tank by two metering pumps Gamma L (Prominent). The scrubbing liquid was recirculated to  
105 the top of the contactor by a centrifugal pump (MDFL from Iwaki) and the liquid flow rate  
106 was controlled by an electromagnetic flowmeter (Promag 10 P from Endress Hauser).

107 A bypass located after the recirculation pump allowed the measurement of the pH,  
108 Redox, temperature and conductivity of the scrubbing liquid by specific probes (Endress  
109 Hauser). The pH and the hypochlorite concentration of the scrubbing liquid, clean water  
110 supply and drain were regulated respectively by the pH, the Redox and the conductivity  
111 measurements. Pressure measurements upstream and downstream the contactor involved two  
112 pressure sensors Cerabar S PMC 71 (Endress Hauser). The  $H_2S$  concentration was  
113 continuously measured upstream ( $[H_2S]_{G,i}$ ) and downstream ( $[H_2S]_{G,o}$ ) the contactor by

114 means of two electrochemical sensors Polytron (Dräger). The H<sub>2</sub>S removal efficiency was  
115 defined as:

116

$$117 \quad \text{Eff} = \frac{[\text{H}_2\text{S}]_{\text{G,i}} - [\text{H}_2\text{S}]_{\text{G,o}}}{[\text{H}_2\text{S}]_{\text{G,i}}} = 1 - \frac{[\text{H}_2\text{S}]_{\text{G,o}}}{[\text{H}_2\text{S}]_{\text{G,i}}} \quad (2)$$

118

## 119 **Results and discussion**

120

### 121 **Influence of the hydrodynamic conditions on the pressure drop and the H<sub>2</sub>S removal**

122

123 Through the transparent PVC pipe contactor, a strong dispersion of the liquid into  
124 small droplets was observed for U<sub>SG</sub> higher than 13-14 m.s<sup>-1</sup>. The ratio L/G, which represents  
125 the ratio of the recirculated liquid mass flow rate and the treated gas mass flow rate, is  
126 generally close to 3 when H<sub>2</sub>S is treated in packed columns (Bonnin, 1991). The pressure  
127 drop ΔP was measured for 600 < Q<sub>G</sub> < 2800 m<sup>3</sup>.h<sup>-1</sup> and 3500 < Q<sub>L</sub> < 8000 L.h<sup>-1</sup> (L/G from 1.1  
128 to 11.2). It could be observed that ΔP strongly increased with U<sub>SG</sub>, since the gas is the  
129 continuous phase, and with a minor extent with U<sub>SL</sub> (Figure 2). This energy loss is partly  
130 transferred to the liquid to achieve a better liquid dispersion and mixing. As a consequence,  
131 when U<sub>SG</sub> increases, mass transfer rate increases, leading to an improvement of the H<sub>2</sub>S  
132 removal efficiency (Figure 3). Hence, a compromise must be realised for the selection of U<sub>SG</sub>  
133 in order to limit the pressure drop to ensure the process economic viability. The pressure drop  
134 per reactor height unit (ΔP/H<sub>r</sub>) could be well correlated to the gas and liquid superficial  
135 velocities U<sub>SG</sub> and U<sub>SL</sub>:

136

137 
$$\frac{\Delta P}{H_r} (\text{Pa.m}^{-1}) = 285.7 \times U_{SG}^{1.68} \times U_{SL}^{0.47} = 11.9 \times U_{SG}^{2.15} \times \left(\frac{L}{G}\right)^{0.47} \quad (3)$$

138

139 The determination coefficient ( $R^2$ ) between the experimental and the predicted  
140 pressure drops is 99.94 %. However, this equation is valid only for this packing geometry and  
141 diameter and should not be used for scale-up.

142 Otherwise, Figure 4 demonstrates that an increase of  $U_{SL}$  (proportional to  $L/G$ ) at a  
143 given gas flow rate induces a significant better  $H_2S$  removal. This evolution could be  
144 attributed to a better hydrodynamic behaviour. Indeed, Sanchez et al. (2007a) demonstrated at  
145 the laboratory scale that  $k_L a^0$  increases with the liquid velocity (or flow rate). Moreover,  $L/G$   
146 increasing implies that more liquid flows in the contactor (the liquid hold-up increases),  
147 which allows to limit the pH and hypochlorite concentration decrease due to the oxidation  
148 reaction. However, increasing the liquid flow rate generates a higher pressure drop and  
149 consumes more electrical power for the recirculation, which leads to a more expensive  
150 operation.

151

## 152 **Influence of the chemical conditions on the $H_2S$ removal**

153

154 Chemical conditions can notably influence the  $H_2S$  removal. Now, no significant  
155 variation of the  $H_2S$  removal was observed when the pH varied between 9.5 and 11 (not  
156 presented here). However, for a pH close to 9.5, the formation of a yellow precipitate of  
157 colloidal sulphur was observed whereas for a pH close to 11, the formation of a white  
158 precipitate of carbonates could be noticed (due to the reaction between NaOH and  $CO_2$   
159 present in atmospheric air). Then, all the results presented in this paper were performed with a  
160 pH ranging between 10 and 10.5 (low and high pH thresholds of the regulation). Figure 4  
161 demonstrates a positive influence of the sodium hypochlorite concentration on the  $H_2S$

162 removal. When the hypochlorite concentration increases, the oxidation kinetics improvement  
 163 favours H<sub>2</sub>S oxidation in the liquid film which enhances the removal efficiency. This result is  
 164 particularly interesting considering that it is a low cost operating solution comparing to an  
 165 increasing of U<sub>SG</sub> and U<sub>SL</sub>. Several experiments were carried out for U<sub>SG</sub> =14.1 m.s<sup>-1</sup>, U<sub>SL</sub> =  
 166 0.093 m.s<sup>-1</sup>, 10 < pH < 10.5 and [ClO<sup>-</sup>] ≈ 3 g.L<sup>-1</sup>, but with [H<sub>2</sub>S]<sub>G,i</sub> varying from 6 to 80 ppmv.  
 167 The H<sub>2</sub>S removal was not significantly different and close to 96 %. The H<sub>2</sub>S removal is  
 168 consequently independent of the inlet concentration. However, one has to keep in mind that  
 169 working with high inlet concentration favours hydroxide anion and hypochlorite  
 170 consumptions in the scrubber. Consequently, the amount of H<sub>2</sub>S treated must be lower than  
 171 twice the amount of hydroxide anion and 4 times the amount of hypochlorite in the scrubbing  
 172 liquid at the inlet. With a classical H<sub>2</sub>S inlet concentration in WWTP of 5-6 ppmv, it is  
 173 therefore possible to reach an H<sub>2</sub>S outlet concentration ranging between 0.1 and 0.2 ppmv,  
 174 which is close to the values that deodorisation unit designers guaranty (Verguet et al., 2008).

175

## 176 **H<sub>2</sub>S removal modelling**

177

178 Assuming a plug flow of the gas phase, in an elementary contactor height (dz in m),  
 179 the H<sub>2</sub>S transferred flow (dN in mol.s<sup>-1</sup>) can be expressed as:

180

$$181 \quad dN = k_L a^0 E ([H_2S]_L^* - [H_2S]_L) S_{col} dz = K_L a^0 \left( \frac{[H_2S]_G}{H_{H_2S}} - [H_2S]_L \right) S_{col} dz \quad (4)$$

182

183  $k_L$  and  $K_L$  are respectively the local and overall liquid mass transfer coefficients (m.s<sup>-1</sup>)  
 184 <sup>1</sup>,  $a^0$  is the volumetric interfacial area (m<sup>2</sup>.m<sup>-3</sup>),  $S_{col}$  the contactor section (m<sup>2</sup>),  $[H_2S]_L^*$  the  
 185 H<sub>2</sub>S concentration in the liquid phase at the gas-liquid interface (mol.m<sup>-3</sup>) and  $[H_2S]_L$  the H<sub>2</sub>S



186 concentration in the bulk of the liquid ( $\text{mol}\cdot\text{m}^{-3}$ ).  $H'_{\text{H}_2\text{S}}$  is the Henry's law constant in water of  
 187  $\text{H}_2\text{S}$  at 293 K ( $= 0,363 \text{ mol L}^{-1} / \text{mol L}^{-1}$ ).  $E$  is the enhancement factor, equal to the rate of  $\text{H}_2\text{S}$   
 188 transferred when the reaction occurs divided by the rate of  $\text{H}_2\text{S}$  transferred when no reaction  
 189 occurs ( $E \geq 1$ ).  $K_L$  is linked to  $k_L$  and  $k_G$  (the local liquid and gas mass transfer coefficients)  
 190 and  $E$  by:

191

$$192 \quad \frac{1}{K_L} = \frac{1}{Ek_L} + \frac{1}{H'_{\text{H}_2\text{S}}k_G} \quad (5)$$

193

194 Oxidation of  $\text{H}_2\text{S}$  by hypochlorite at basic pH is fast and happens in the liquid film at  
 195 the vicinity of the gas-liquid interface (Danckwerts, 1970). It means that  $\text{H}_2\text{S}$  is completely  
 196 consumed in the liquid film by the oxidation reaction, leading to  $E \gg 1$  and  $[\text{H}_2\text{S}]_L \approx 0$ . In  
 197 this case, the first ratio of the right-hand terms of the Equation (5) may become negligible  
 198 (instantaneous surface reaction) showing that all the resistance for mass transfer can be  
 199 located in the gas film. However, the results demonstrated that the removal efficiency  
 200 increased with the hypochlorite concentration, i.e. with the reaction kinetics, which clearly  
 201 shows that a part of the resistance for mass transfer is still located in the liquid film and can  
 202 not be neglected. Consequently,  $E$  must be estimated and depends on two dimensionless  
 203 numbers: the Hatta number for a 2<sup>nd</sup> order kinetics ( $Ha$ ) and the enhancement factor for an  
 204 infinitely fast reaction ( $E_i$ ) (Danckwerts, 1970):

205

$$206 \quad E = Ha = \frac{\sqrt{D_{\text{H}_2\text{S},w} [\text{ClO}^-] k_{\text{ox}}}}{k_L} \quad \text{and} \quad E_i = \frac{D_{\text{ClO}^-,w} [\text{ClO}^-]}{D_{\text{H}_2\text{S},w} [\text{H}_2\text{S}]_L^*} \quad (6)$$

207

208  $k_{ox}$  is the apparent kinetics constant ( $L.mol^{-1}.s^{-1}$ ) of the oxidation reaction and  $D_{H_2S,w}$   
 209 and  $D_{ClO^-,w}$  are respectively the diffusion coefficients of  $H_2S$  ( $1.6 \cdot 10^{-6} m^2.s^{-1}$ ) and  $ClO^-$  ( $1.3$   
 210  $10^{-6} m^2.s^{-1}$ ) in water. The Hatta number represents the maximum pollutant conversion in the  
 211 liquid film compared with its maximum transport through the film.

212 According to usual hypochlorite concentrations in the scrubbing liquid ( $> 0.1 g.L^{-1}$ ),  
 213 hypochlorite is in great excess comparing to hydrogen sulphide at the gas-liquid interface. In  
 214 this case, the kinetics is pseudo-first order and the enhancement factor  $E$  is equal to  $Ha$   
 215 considering that this last number is large (see Table 1) but significantly lower  $E_i$  (which is in  
 216 the range 4 000-92 000 at the scrubber inlet, depending on  $[ClO^-]$  and  $[H_2S]_{G,i}$ ).

217 The amount of hydrogen sulphide treated in the scrubber is negligible comparing to  
 218 the amount of hypochlorite at the inlet. The hypochlorite concentration, and by the way the  
 219 Hatta number, are consequently constant in the scrubber, assuming that  $k_{ox}$  does not depend in  
 220 a great extent of the pH which should decrease due to the hydroxide anion consumption.  
 221 Therefore:

222

$$223 \quad \frac{1}{K_L} = \frac{1}{k_L \sqrt{D_{H_2S,w} [ClO^-] k_{ox}}} + \frac{1}{H'_{H_2S} k_G} = \frac{1}{\sqrt{D_{H_2S,w} [ClO^-] k_{ox}}} + \frac{1}{H'_{H_2S} k_G} \quad (7)$$

224

225 According to the Equation (7), the Equation (4) can be rewritten:

226

$$227 \quad dN = \frac{a^0}{\frac{1}{\sqrt{D_{H_2S,w} [ClO^-] k_{ox}}} + \frac{1}{H'_{H_2S} k_G}} \frac{[H_2S]_G}{H'_{H_2S}} S_{col} dz \quad (8)$$

228

229 By integration considering the height of the scrubber ( $H_r$ ), an analytical equation of the  
 230 overall flow of  $H_2S$  transferred is deduced:

$$231 \quad N = \frac{a^0}{\frac{H_{H_2S}}{\sqrt{D_{H_2S,w} [ClO^-] k_{ox}}} + \frac{1}{k_G}} \frac{[H_2S]_{G,i} - [H_2S]_{G,o}}{\ln([H_2S]_{G,i} / [H_2S]_{G,o})} S_{col} H_r \quad (9)$$

232  
 233 The gas phase mass balance between the inlet and the outlet leads after rearrangement  
 234 to the equation (10):

$$235 \quad \text{Eff} = 1 - \frac{[H_2S]_{G,o}}{[H_2S]_{G,i}} = 1 - \exp \left( - \frac{a^0}{\frac{H_{H_2S}}{\sqrt{D_{H_2S,w} [ClO^-] k_{ox}}} + \frac{1}{k_G}} \frac{H_r}{U_{SG}} \right) \quad (10)$$

236  
 237 This equation shows that the removal efficiency depends on the liquid dispersed state  
 238 (through  $a^0$ ), the turbulences in the gas phase (through  $k_G$ ) and the oxidation kinetics (through  
 239 the product of  $[ClO^-]$  and  $k_{ox}$ ). Moreover, the efficiency is not influenced by the absorption  
 240 rate and the inlet  $H_2S$  concentration while hypochlorite and hydroxide anions are in excess. At  
 241 the laboratory scale (Sanchez et al., 2007b), and considering that the surface tension, density  
 242 and viscosity of the scrubbing liquid are constant in the scrubber, hydrodynamic study  
 243 demonstrated that  $a^0$  is a power law function of the superficial velocities:  $a^0 = A \cdot U_{SG}^\alpha \cdot U_{SL}^\beta$   
 244 with  $A$ ,  $\alpha$  and  $\beta$  three constants. Then, the Equation (10) can be rewritten:

$$245 \quad \text{Eff} = 1 - \exp \left( - \frac{A \cdot U_{SG}^{\alpha-1} \cdot U_{SL}^\beta}{\frac{H_{H_2S}}{\sqrt{D_{H_2S,eau} [ClO^-] k_{ox}}} + \frac{1}{k_G}} H_r \right) \quad (11)$$

246

247  $k_G$  should be influenced by  $U_{SG}$ . However, this variation can be neglected assuming  
 248 that  $U_{SG}$  has been slightly modified (from 14.1 to 18.6  $m.s^{-1}$ ). Therefore,  $k_G$  can be considered  
 249 as a constant. In the equation (11),  $A$ ,  $\alpha$ ,  $\beta$ ,  $k_G$  and  $k_{ox}$  are unknown. Due to the high  $H_2S$   
 250 oxidation kinetics,  $k_{ox}$  should be in the range  $10^6 - 5 \times 10^8 L.mol^{-1}.s^{-1}$ . Consequently,  $A$ ,  $\alpha$ ,  $\beta$   
 251 and  $k_G$  have been determined (Table 1) for different values of  $k_{ox}$  in this range by numerical  
 252 fitting by the least square method trying to minimise the residual:

253

$$254 \quad \text{Residual} = \frac{1}{M} \sum_{i=1}^M \left( \frac{\text{Eff}_{\text{exp}} - \text{Eff}_{\text{mod}}}{\text{Eff}_{\text{mod}}} \right)^2 \quad \text{with } M = 18 \text{ the number of experimental data} \quad (12)$$

255

256 The model correlates with a good agreement the experimental results whatever the  
 257 value of  $k_{ox}$  selected with an average error lower than 1 % (Table 1). It demonstrates that  
 258 assuming  $k_G$  as a constant is not aberrant. When the selected value of  $k_{ox}$  decreases,  $a^0$   
 259 increases to compensate the lower enhancement by chemical reaction. At the laboratory scale,  
 260 for similar superficial velocities, the average interfacial area and gas side mass transfer  
 261 coefficient were respectively in the range of 1500-2000  $m^2.m^{-3}$  and 0.1-0.2  $m.s^{-1}$ . These  
 262 values would be reached at the semi-industrial scale for a  $k_{ox}$  equal to  $6 \times 10^6 L.mol^{-1} s^{-1}$ .  
 263 However, this value should be considered with care since the scale difference between the  
 264 laboratory and this study (and consequently the difference of Reynolds Number) may lead to  
 265 significant variations of the ranges of  $a^0$  and  $k_G$ .

266

### 267 **Pressure drop and removal efficiency simulations**

268

269 Using Equations (3) and (11), simulations of the pressure drop and the removal  
 270 efficiency for different operating conditions can be achieved. In order to limit the operating

271 cost of the process, a low value of  $U_{SG}$  (but sufficient to insure a strong liquid dispersion  $\Rightarrow$   
272  $U_{SG} > 13 \text{ m.s}^{-1}$ ) must be selected. Consequently, two simulations have been realised at 13.3  
273 and  $14.1 \text{ m.s}^{-1}$  (respectively  $1500$  and  $1600 \text{ m}^3.\text{h}^{-1}$ ) using  $k_{ox} = 6 \times 10^6 \text{ L.mol}^{-1}.\text{s}^{-1}$  (Figure 5).  
274 The choice of the quintet A, a, b,  $k_G$  and  $k_{ox}$  does not influence the results of the simulation.  
275 Simulations confirm that the removal efficiency increases significantly with the hypochlorite  
276 concentration when lower than  $3 \text{ g.L}^{-1}$ . Moreover, the removal efficiency increases strongly  
277 with the L/G ratio until 5. Using a hypochlorite concentration and a L/G ratio higher than 3  
278  $\text{g.L}^{-1}$  and 5 is not necessary whatever the gas superficial velocity. Using such operating  
279 conditions, the removal efficiency reaches 95 % for a moderate pressure drop which remains  
280 lower than 3500-4000 Pa (maximal pressure drop to insure the process economic viability).

281

## 282 **CONCLUSION**

283

284 A new compact chemical scrubber was implemented in a WWTP. Results showed that  
285 both hydrodynamic and chemical conditions significantly influence the  $\text{H}_2\text{S}$  removal. A  
286 model was developed to predict the pressure drop and the  $\text{H}_2\text{S}$  removal at any given operating  
287 condition. An interesting economic compromise was deduced for a moderate gas velocity and  
288 a high hypochlorite concentration. The new packing has not been optimised yet and some  
289 improvement of the structure would certainly offer a lower pressure drop for a similar mass  
290 transfer rate. To insure a high level of deodorisation, two scrubbers in series could be  
291 implemented but the increasing of the pressure drop must be taken into account.

292

293 **NOMENCLATURE**

294	[A]	concentration of the compound A
295	A, $\alpha$ and $\beta$	coefficients determined by numerical resolution
296	$a^0$	interfacial area related to the volume of the contactor ( $\text{m}^2 \cdot \text{m}^{-3}$ )
297	$D_{\text{H}_2\text{S},\text{w}}$	diffusion coefficient of $\text{H}_2\text{S}$ in water ( $\text{m}^2 \cdot \text{s}^{-1}$ )
298	dz	infinitesimal height of contact (m)
299	E	enhancement factor
300	$E_i$	enhancement factor for an infinitely fast reaction
301	Eff	$\text{H}_2\text{S}$ removal efficiency (%)
302	Ha	Hatta number
303	$H'_{\text{H}_2\text{S}}$	$\text{H}_2\text{S}$ Henry's constant in water
304	$H_r$	height of the contactor (m)
305	$k_G$ ( $K_G$ )	(overall) gas phase mass transfer coefficient ( $\text{m} \cdot \text{s}^{-1}$ )
306	$k_L$ ( $K_L$ )	(overall) liquid phase mass transfer coefficient ( $\text{m} \cdot \text{s}^{-1}$ )
307	$k_{G a^0}$ ( $K_{G a^0}$ )	(overall) gas phase volumetric mass transfer coefficient ( $\text{s}^{-1}$ )
308	$k_{L a^0}$ ( $K_{L a^0}$ )	(overall) liquid phase volumetric mass transfer coefficient ( $\text{s}^{-1}$ )
309	$k_{\text{ox}}$	kinetics constant of $\text{H}_2\text{S}$ oxidation by hypochlorite at basic pH ( $\text{L} \cdot \text{mol}^{-1} \cdot \text{s}^{-1}$ )
310	L/G	ratio of liquid and gas mass flow rates
311	N (dN)	(infinitesimal) flow of $\text{H}_2\text{S}$ transferred ( $\text{mol} \cdot \text{s}^{-1}$ )
312	$Q_G$ ( $Q_L$ )	gas (liquid) volume flow rates ( $\text{m}^3 \cdot \text{h}^{-1}$ or $\text{m}^3 \cdot \text{s}^{-1}$ )
313	$S_{\text{col}}$	section of the contactor ( $\text{m}^2$ )
314	$U_{SG}$ ( $U_{SL}$ )	gas (liquid) superficial velocity ( $\text{m} \cdot \text{s}^{-1}$ )
315	WWTP	Waste Water Treatment Plant
316		
317		

318 Greek letters

319  $\Delta P$  pressure drop (Pa)

320 Indices

321 i inlet

322 G gas

323 L liquid

324 o outlet

325 \* interface

326

327 **REFERENCES**

- 328  
329 Biard, P.-F., A. Couvert, C. Renner, J.-P. Levasseur, "Assessment and Optimisation of VOC  
330 Mass Transfer Enhancement by Advanced Oxidation Process in a Compact Wet  
331 Scrubber," *Chemosphere* **77**, 182-187 (2009a).
- 332 Biard, P.-F., A. Couvert, C. Renner, P. Zozor, S. Bassivière, J.-P. Levasseur, "Hydrogen  
333 Sulphide Removal in Waste Water Treatment Plant by Compact Oxidative Scrubbing in  
334 Aquilair Plus<sup>TM</sup> Process," *Water Practice and Technology* **4**, doi:10.2166/wpt.2009.2023  
335 (2009b).
- 336 Bonnin, C., "Les Sources De Nuisances Olfactives Dans Les Stations De Traitement Des  
337 Eaux Usées Résiduaire, Et Leur Traitement Par Lavage À L'eau Chlorée En Milieu  
338 Basique," Thesis of the Université de Rennes I, Ecole Nationale Supérieure de Chimie de  
339 Rennes (1991).
- 340 Busca, G., P. Chiara, "Technologies for the Abatement of Sulphide Compounds from Gaseous  
341 Streams: A Comparative Overview," *Journal of Loss Prevention in the Process Industries*  
342 **16**, 363-371 (2003).
- 343 Chen, L., J. Huang, C.-L. Yang, "Absorption of H<sub>2</sub>S in NaOCl Caustic Aqueous Solution,"  
344 *Environmental Progress* **20**, 175-181 (2001).
- 345 Couvert, A., C. Sanchez, A. Laplanche, C. Renner, "Scrubbing Intensification for Sulphur and  
346 Ammonia Compounds Removal," *Chemosphere* **70**, 1510-1517 (2008).
- 347 Danckwerts, P.V., "Gas-Liquid Reactions," MacGraw Hill, New-York (1970).
- 348 Gostelow, P., S. A. Parsons, R. M. Stuetz, "Odour Measurements for Sewage Treatment  
349 Works," *Water Research* **35**, 579-597 (2001).
- 350 Sanchez, C., A. Couvert, C. Renner, "Device for Treating a Gaseous Effluent Loaded with  
351 Odorant Compounds Using a Three-Dimensional Mesh, Corresponding Installation and  
352 Process," WO 2007/063104 A1, OTV, France (2007a).
- 353 Sanchez, C., A. Couvert, A. Laplanche, C. Renner, "Hydrodynamic and Mass Transfer in a  
354 New Co-Current Two-Phase Flow Gas-Liquid Contactor," *Chemical Engineering Journal*  
355 **131**, 49-58 (2007b).
- 356 Sanchez, C., A. Couvert, A. Laplanche, C. Renner, "New Compact Scrubber for Odour  
357 Removal in Wastewater Treatment Plants," *Water Science and Technology* **54**, 45-52  
358 (2007c).



359 Verguet, J., E. Guibelin, K. Kaczor, "Performances Du Traitement Des Odeurs En Usine  
360 D'épuration : Ce Que L'On Est En Droit D'attendre," L'eau, l'Industrie, les Nuisances **313**,  
361 49-51 (2008).  
362  
363

364 **Figure captions**

365

366 Figure 1. Set-up scheme.

367 Figure 2. Pressure drop inside the scrubber versus  $U_{SG}$  for different  $U_{SL}$  ( $Q_L = 3.5, 5.0, 6.5$

368 and  $8.0 \text{ m}^3 \cdot \text{h}^{-1}$ ).

369 Figure 3.  $\text{H}_2\text{S}$  removal and pressure drop versus  $U_{SG}$  ( $L/G = 3.5$  ;  $40 < [\text{H}_2\text{S}]_{G,i} < 50$  ppmv ;

370  $[\text{ClO}^-] \approx 1.5 \text{ g} \cdot \text{L}^{-1}$ ;  $10 < \text{pH} < 10.5$ ).

371 Figure 4.  $\text{H}_2\text{S}$  removal and pressure drop versus  $L/G$  ( $U_{SG} = 15 \text{ m} \cdot \text{s}^{-1}$  ;  $40 < [\text{H}_2\text{S}]_{G,i} < 50$  ppmv

372 ;  $10 < \text{pH} < 10.5$  ).

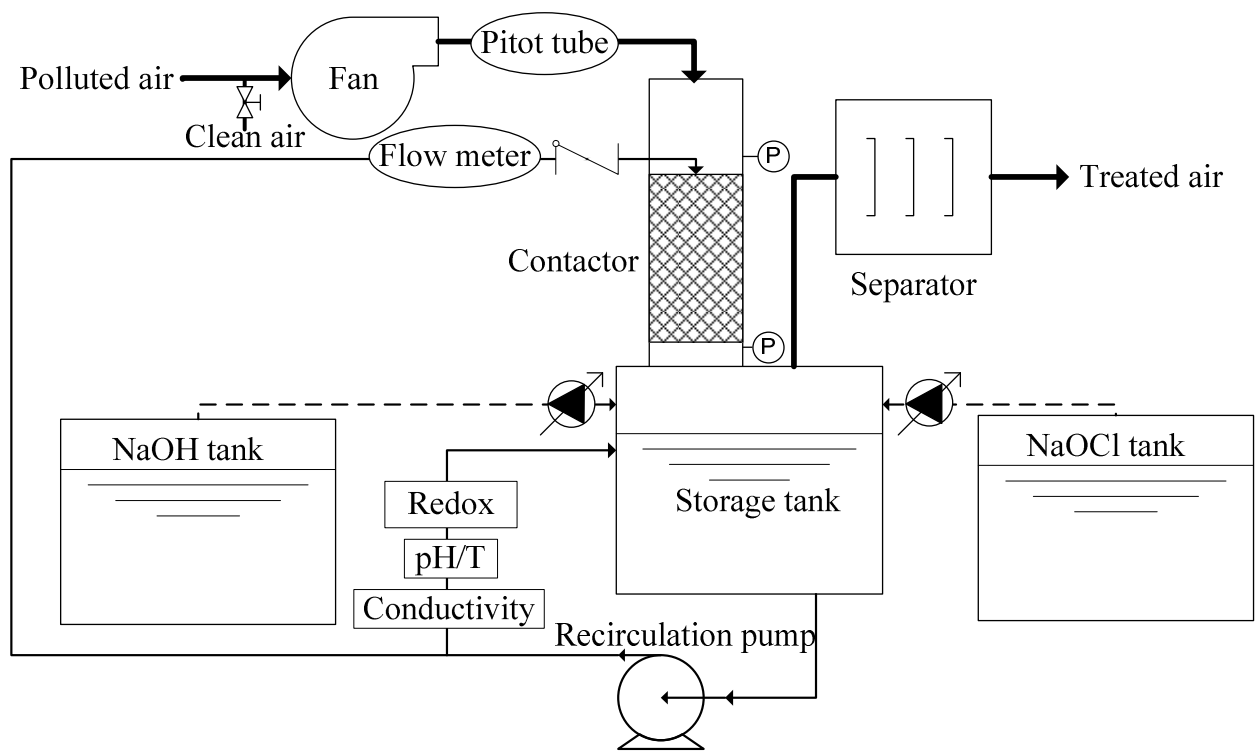
373 Figure 5. Simulation of  $\text{H}_2\text{S}$  removal and pressure drop for two gas superficial velocities ( $U_{SG}$

374 =  $13.3 \text{ m} \cdot \text{s}^{-1}$  ( $Q_G = 1500 \text{ m}^3 \cdot \text{h}^{-1}$ ) and  $14.1 \text{ m} \cdot \text{s}^{-1}$  ( $Q_G = 1600 \text{ m}^3 \cdot \text{h}^{-1}$ )) for  $2 \leq L/G \leq 6$  and  $1 \leq$

375  $[\text{ClO}^-] \leq 4 \text{ g} \cdot \text{L}^{-1}$ .

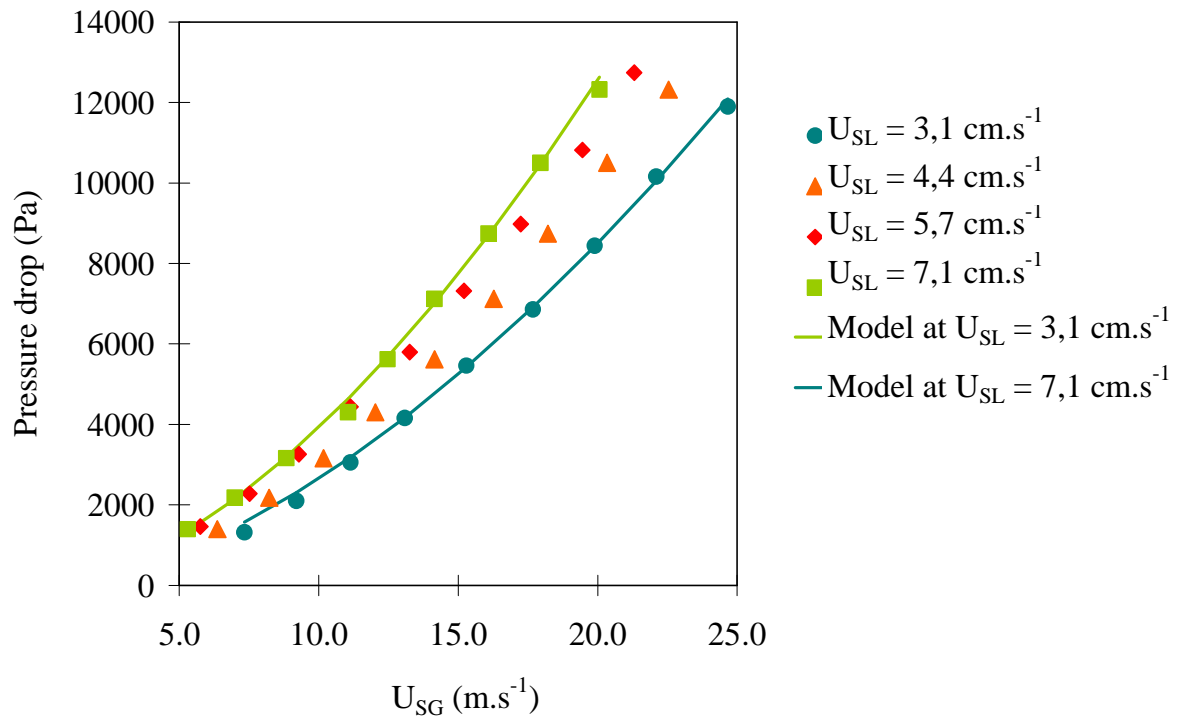
376

377



378  
 379  
 380

Figure 1

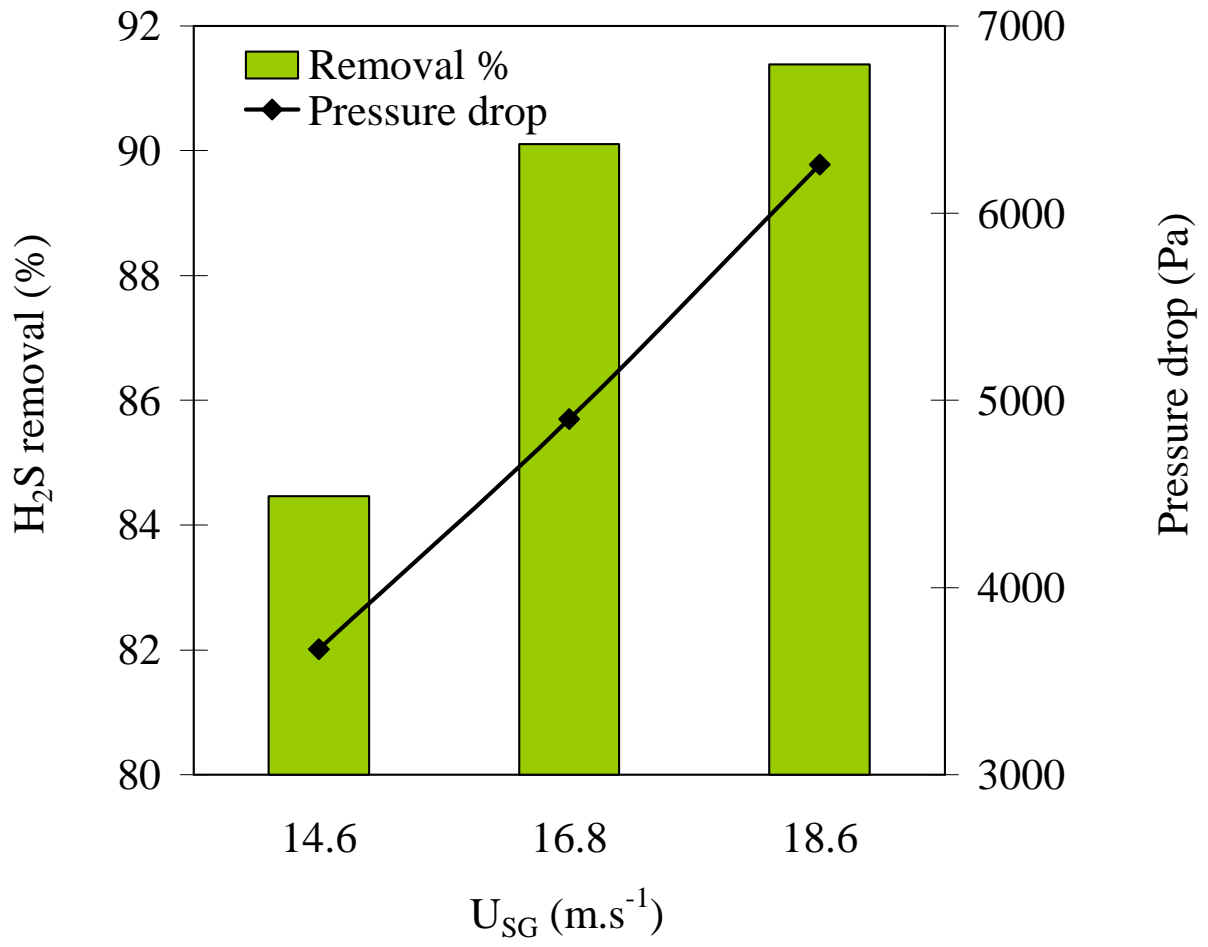


381

382

383

Figure 2



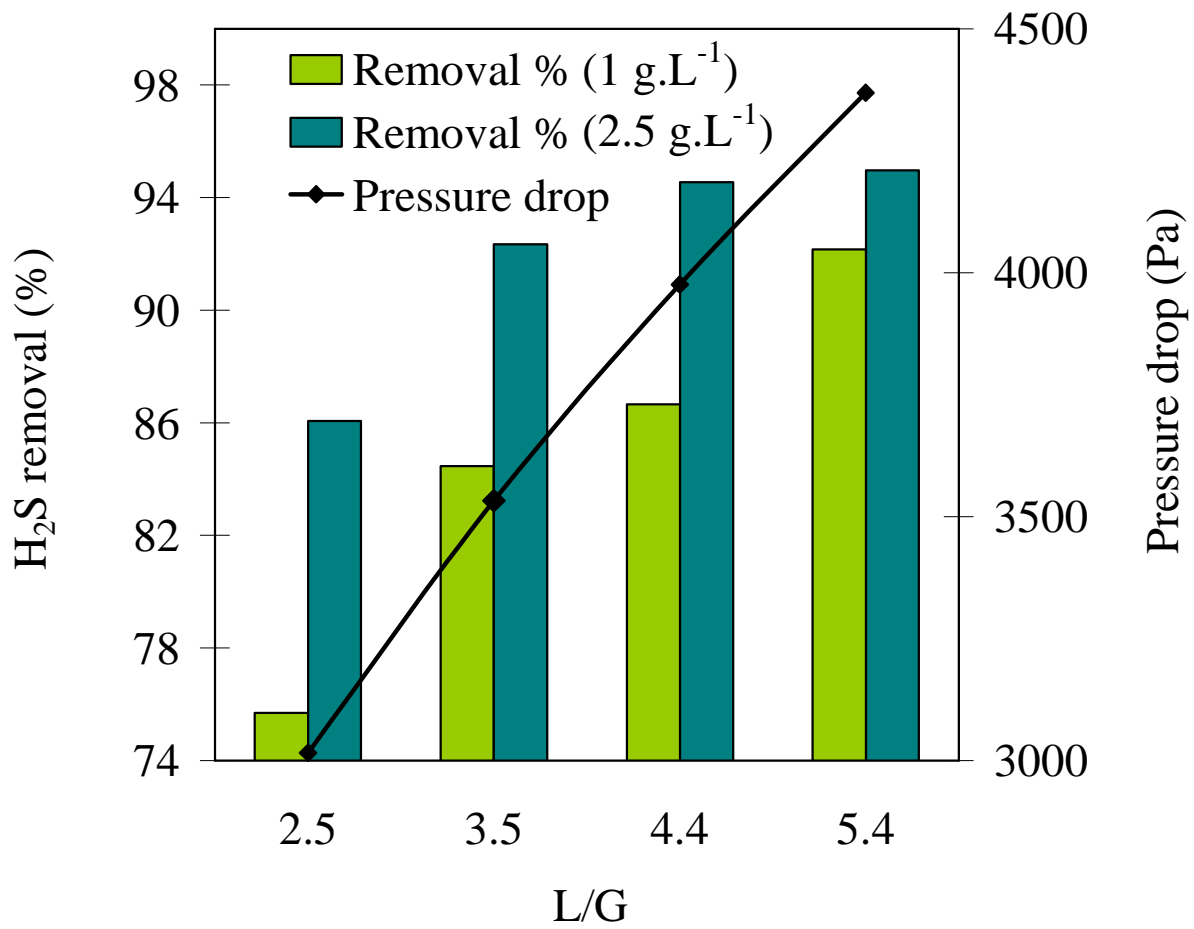
384

385

386

387

Figure 3

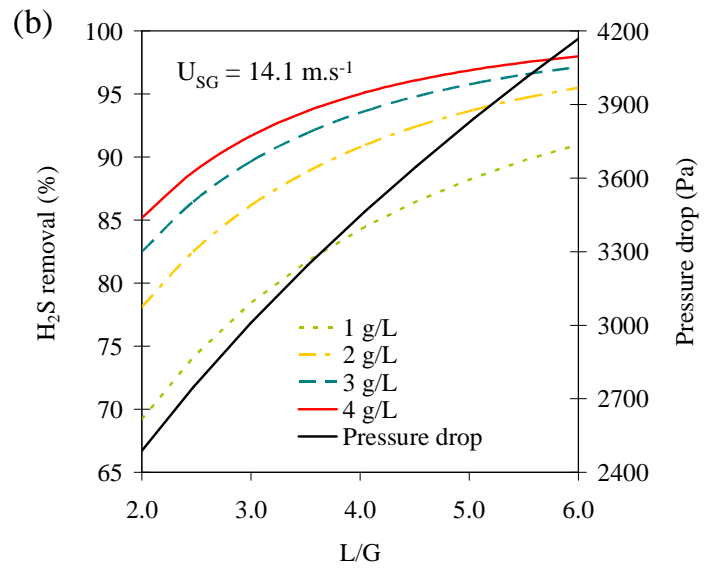
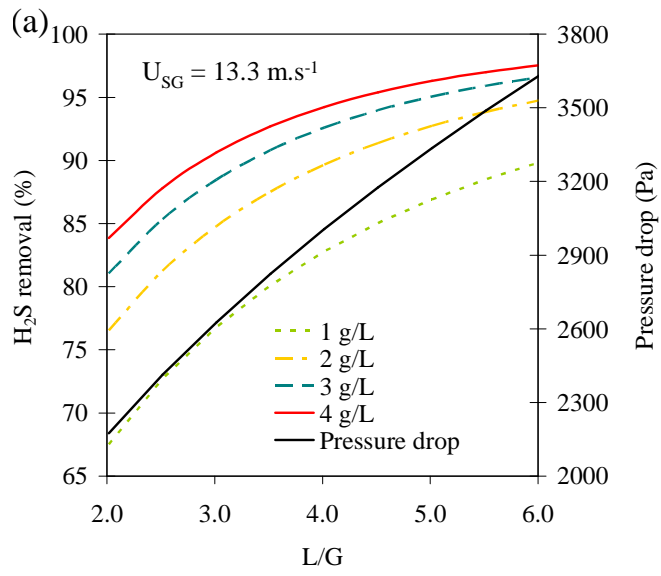


388

389

390

Figure 4



391

392

393

Figure 5

394 Table 1. Hatta range values (considering  $k_L = 10^{-4} \text{ m.s}^{-1}$ ) and results of the numerical fitting  
 395 for several values of  $k_{ox}$ .

396

$k_{ox} (\text{L.mol}^{-1}.\text{s}^{-1})$	$1.0 \times 10^6$	$6.0 \times 10^6$	$1.0 \times 10^7$	$1.0 \times 10^8$	$5.0 \times 10^8$
Hatta range	80-116	195-285	250-370	790-1 160	1 770-2 600
A	205.06	146.98	118.43	47.67	25.85
$\alpha$	1.61	1.45	1.44	1.37	1.21
$\beta$	0.59	0.61	0.61	0.62	0.64
$k_G (\text{m.s}^{-1})$	0.14	<b>0.24</b>	0.31	0.85	2.07
$a^0$ average ( $\text{m}^2.\text{m}^{-3}$ )	3 636	<b>1 575</b>	1 225	398	135
$k_G a^0$ average ( $\text{s}^{-1}$ )	510	<b>378</b>	380	338	277
$R^2$ (%)	97.44	97.97	97.99	98.06	97.94
Average error (%)	0.83	0.72	0.71	0.67	0.68

397

398